Accepted Manuscript

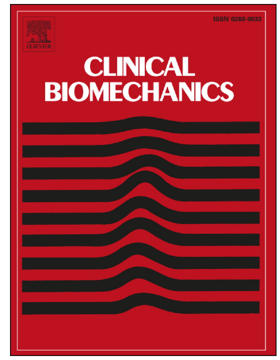

Quantifying the in vivo quasi-static response to loading of sub-dermal tissues in the human buttock using magnetic resonance imaging

Rami M.A. Al-Dirini, John Nisyrios, Matthew P. Reed, Dominic Thewlis

PII: S0268-0033(17)30211-5
DOI: doi:10.1016/j.clinbiomech.2017.09.017
Reference: JCLB 4392

To appear in: *Clinical Biomechanics*

Received date: 17 October 2016
Accepted date: 27 September 2017

Title: Quantifying the *in vivo* Quasi-static Response to loading of Sub-dermal Tissues in the Human Buttock using Magnetic Resonance Imaging

*Rami M A Al-Dirini[1], John Nisyrios[2], Matthew P Reed[3], Dominic Thewlis[4]

* Corresponding author:

Email: rami.aldirini@flinders.edu.au

[1] Medical Devices Research Institute, College of Science and Engineering, Flinders University, Adelaide, SA 5001, Australia

[2] Fowler Simmons Radiology, Adelaide, SA 5000, Australia

[3] University of Michigan Transportation Research Institute, University of Michigan, Ann Arbor, MI 48109, USA

[4] Centre for Orthopaedic & Trauma Research, Faculty of Health and Medical Sciences, the University of Adelaide, Adelaide, SA 5000, Australia

Word count: 248 words

Abstract

Background: The design of seating systems to improve comfort and reduce injury would benefit from improved understanding of the deformation and strain patterns in soft tissues, particularly in the gluteal region.

Methods: Ten healthy men were positioned in a semi-recumbent posture while their pelvic and thigh region was scanned using a wide-bore magnetic resonance imaging (MRI) scanner. Independent measurements of deformation for muscles and fat were taken for the transition from non-weight-bearing to weight-bearing loads in three stages. A weight-bearing load was achieved through having the subject supported by a flat, rigid surface. A non-weight-bearing condition was achieved by removing the support under the left buttock, leaving all soft tissue layers undeformed. An intermediate condition partially relieved the subject's left buttock by lowering the support relative to the pelvis by 20 mm, which left the buttock partially deformed. For each of these conditions, the thicknesses of muscle and fat tissues below the ischial tuberosity and the greater trochanter were measured from the MRI data.

Findings: In this dataset, the greatest soft tissue deformation took place below the ischial tuberosity, with muscles (mean =17.7mm, SD = 4.8mm) deforming more than fat tissues (mean = 4.3mm, SD = 5.6mm). Muscles deformed through both steps of the transition from weight-bearing to non-weight-bearing conditions, while subcutaneous fat deformed little after the first transition from non-weight-bearing to partial-weight-bearing. High inter-subject variability in muscle and fat tissue strains was observed,

Interpretation: Our findings highlight the importance of considering inter-subject variability when designing seating systems.

Keywords: Magnetic resonance imaging (MRI), muscle, quantification and estimation, sitting, soft tissue deformation, sitting discomfort, pressure sores

Word count: 3,788 words

1 Introduction

Sitting for extended periods of time can compromise the health of gluteal soft tissues and may lead to discomfort or even injury (Stockton and Parker, 2002; Wall, 2000). As a person settles into a weight-bearing sitting posture, muscle and fat tissues in the gluteal region undergo large deformations. The high mechanical loads and the associated large soft tissue deformation below bony structures such as the ischial tuberosities are major factors contributing to sitting related discomfort and injury (Linder-Ganz et al., 2007; Shabshin et al., 2010).

Soft tissue response to mechanical loading has been studied using cadaveric samples (Untaroiu et al., 2005; Untaroiu and Lu, 2013) and animal models (Gefen, 2008b; Linder-Ganz et al., 2006; Linder-Ganz and Gefen, 2004). These models help explain the phenomenological behaviour of soft tissues under loading, but they may not be an accurate guide to the *in vivo* behaviour of sub-dermal tissue layers of the human body (Makhsous and Lin, 2009), due to differences in mechanical behaviour between animal models or cadavers and soft tissues in living humans (Salcido et al., 2007).

Current non-invasive technology cannot measure the sub-dermal tissue strains in response to mechanical loading, *in vivo*. Alternately, the *in vivo* behaviour, specifically deformation, of soft tissues can be used as an indirect measure of the mechanical response (strains) to loading (Shabshin et al., 2010b). Deformation of muscle and fat tissues for seated humans have been measured, *in vivo,* using medical imaging technologies such as ultrasound (Makhsous et al., 2008), Computer Tomography (CT) (Vannah and Childress, 1996) or Magnetic Resonance Imaging (MRI) (Linder-Ganz et al., 2007; Makhsous et al., 2011). However, the majority of previous *in vivo* measurements for gluteal tissue deformation have been limited to single subjects (Makhsous et al., 2007; Sonenblum et al., 2013; Then et al., 2007; Todd and Thacker, 1994). A few studies (Linder-Ganz and Gefen, 2007; Makhsous et al., 2011) have been conducted on larger samples, yet subjects were either lean or slightly overweight (BMI between 18 $kg.m^{-2}$ and 26 $kg.m^{-2}$), and single measurements were taken to describe the entire transition from non-weight-bearing to weight-bearing sitting postures (Al-Dirini et al., 2015).

Access to data describing the deformation history throughout the transition between the extreme loading conditions may help develop a comprehensive understanding of how muscles and fat tissues deform under various sitting loads. Previous studies on gluteal tissue deformation have mostly focused on measuring the deformation, on a rigid seat, from the underformed to the fully deformed states, or vice versa, with little attention given to the intermediate deformation states. However, people mostly sit on some deformable surface/support (cushion), in which gluteal tissues will unlikely achieve the fully deformed state. Instead, soft tissues are more likely to become only partially deformed. Recent research by Sonenblum et al (2015), Call et al (2017) and Brienza et al (2017) have focused on the partially deformed state of gluteal tissues when sitting on deformable cushions. However, to date, data describing the *in vivo*, quasi-static deformation of gluteal tissues from the underformed to the fully deformed states (including intermediate deformation states) have only been published in single-subject studies or for loads that are too small compared to those experienced during sitting. Hence, the aim of this study was to quantify, using MRI scanning, the *in vivo*, quasi-static, compressive deformation of gluteal muscle and fat tissues for a diverse cohort individuals, with focus on tissues below the ischial tuberosity and the greater trochanter. We hypothesised that the *in vivo* response of muscles under quasi-static loads representative of typical sitting are different than those of fat tissues.

2 Methods

2.1 Participants

Ten healthy men within a diverse range of stature and body mass were recruited for this study (Table 1). To be included in this study, subjects had to be men between 18 and 65 years old. Subjects with a history of osteoporosis, arthritis, epilepsy, neuromotor disability and/or dysfunction, joint pathology, back pain or any back related disease were excluded from the study. Since MRI scanning was used in this study, subjects with metallic implants and/or devices (including pacemakers) were also excluded. Due to the spatial constraints of the MRI scanner's dimensions, volunteers with statures greater than 182 cm were also excluded. The protocol for this study was approved by the Human Ethics Committee at the University of South Australia (protocol number: 0000031205) and all participants provided written informed consent.

2.2 Image Data Collection

Each subject wore thin shorts and positioned themselves in a semi-recumbent posture while the pelvic and thigh region of their body was scanned using a wide-bore MRI scanner (General Electric 450W GEM - 1.5 Tesla). The experiment posture was chosen as the least reclined that the scanner bore could accommodate. The subject's posture was supported by wooden boards placed under the buttocks and cushions placed behind the back and under the knees (Figure 1). In the sagittal plane, the angle of the back support surface was 135^{o} to forward horizontal (45˚ back support sagittal angle). The lower-extremity support produced a sagittal thigh angle of approximately 60º (120˚ thigh to lower leg angle), also measured in the sagittal plane. The buttock area was supported by a pair of horizontal, flat, rigid boards, one under each buttock. Due to the reclined posture, a head support was provided. A belt was strapped around the subject's knees to prevent body movement during the scans (Figure 1.a). To measure soft tissue deformation throughout the transition from non-weight-bearing to weight-bearing postures, each subject was exposed to three loading conditions and a scan was taken for each of these conditions. In the first scan, the subject sat in a weight-bearing posture, with the left and right buttocks deformed by the subject's weight (Figure 1.d). The second scan was taken after removing a 10-mm wooden block under the subject's left buttock, which left it partially deformed (Figure 1.e). In the final scan, the non-weight-bearing posture was simulated by removing two additional wooden blocks under the left buttock, leaving all soft tissue layers undeformed (Figure 1.f). Subjects were instructed to actively try to stay level as blocks were removed. Each subject remained in each posture (after the blocks were removed) for approximately five to six minutes before the scanning started. A proton density sequence with inter-slice interval of 10 mm (8-mm slices with 2-mm gaps) in the transverse plane was used for all scans. The fully deformed and the fully undeformed conditions for each subject were also scanned in the sagittal direction at 10-mm intervals (8-mm slices and 2-mm gaps) to compensate for any loss of information due to the relatively large inter-slice intervals in the transverse direction. The total scanning time for each subject was less than 60 minutes, with each scan taking between three and six minutes.

2.3 Deformation and Posture Measurements from MRI Scans

Measurements of the pelvis orientation were taken to ensure that subjects did not make major postural changes between scans. Pelvic orientation measurements were taken in the plane of the transverse MRI slices showing the ischial tuberosities. Pelvic tilt in the frontal plane was defined as the angle between the horizontal and the line passing through the right and left ischial tuberosities (Figure 2). This was repeated for weight-bearing, partial-weight-bearing and non-weight-bearing conditions. The change in the pelvic tilt was taken relative to the full-weight-bearing condition.

The orientation of the left side of the pelvis was measured as the angle between the line passing through the femoral head and the pubic symphysis and the seat surface. This angle was measured in the transverse and sagittal planes (Figure 2).

Muscle and subcutaneous fat tissue thicknesses below the left ischial tuberosity and the left greater trochanter were taken in the transverse plane that included the most inferior points of these bony structures (Figure 2). If the left ischial tuberosity or the left greater trochanter was captured by more than one MRI slice, a mean value for soft tissue thicknesses was calculated based on measurements from each slice. This procedure was repeated for each loading condition. Muscle and subcutaneous fat tissue deformations from the deformed to the undeformed conditions ($\Delta T_{muscle\_MRI\_full}$ and $\Delta T_{fat\_MRI\_full}$) were defined as the difference between the undeformed and the fully deformed muscle and fat thicknesses, respectively. Similarly, partial deformations of muscle ($\Delta T_{muscle\_MRI\_partial}$) and subcutaneous fat tissues ($\Delta T_{fat\_MRI\_partial}$) were defined as the difference between the undeformed and the partially deformed thicknesses.

The Green-Lagrange strains in muscle (ε_{muscle} (GL)) and subcutaneous fat tissues (ε_{fat} (GL)) were estimated using muscle (λ_{muscle} – see Equation 1) and subcutaneous fat tissues (λ_{fat} – see

Equation 2) stretch ratios as per (Equations 3 and 4). Coefficients of variations (CV) were also calculated for muscle and fat MRI estimated strains (Equation 5).

$$\lambda_{muscle} = \frac{T_{Muscle_{deformed\_IT}}}{T_{Muscle_{undeformed\_IT}}} \quad (1)$$

$$\lambda_{fat} = \frac{T_{fat_{deformed\_IT}}}{T_{fat_{undeformed\_IT}}} \quad (2)$$

$$\varepsilon_{\text{fat (GL)}} = \frac{1}{2}\left(\lambda_{fat}{}^{2} - 1\right) \quad (3)$$

$$\varepsilon_{\text{muscle (GL)}} = \frac{1}{2}\left(\lambda_{muscle}{}^{2} - 1\right) \quad (4)$$

$$CV = \frac{standard\ deviation}{mean} \quad (5)$$

3 Results

3.1 Pelvic Tilt and Orientation

The change in the pelvic tilt in the frontal plane was mostly negative indicating the subjects in most cases lifted their left buttock after the support under their left buttock was removed. With the exception of three subjects, the change in pelvic tilt for most subjects was less than 6^{o} of the full-weight-bearing condition (Table 3). Subjects 1 and 5 had relatively large changes in pelvic tilt for both the partial- and the non-weight-bearing conditions.

The pelvic orientation relative to the seat surface ranged between 23.0^{o} and 32.8^{o} in the transverse plane (Φ), and between 52.8^{o} and 88.7^{o} in the sagittal plane (β) (Table 3). It was not possible to measure the pelvis orientation for one subject (subject 2) due to high distortion in the MRI scans near the femoral head and the pubic symphysis.

3.2 Deformation measurements from MRI scans

Measurements from MRI data showed that muscles and subcutaneous fat tissues of all subjects deformed the most below the ischial tuberosity, and that tissues seem to be displaced in the lateral direction when the blocks were removed. For the study cohort, the mean (SD) total deformation (fully deformed → undeformed) of muscles and subcutaneous fat tissues below the ischial tuberosity were 17.7 mm (4.8 mm) and 4.3 mm (5.6 mm) respectively. The largest deformations relative to the initial total soft tissue thicknesses were also below the ischial tuberosity with 36.0% for subcutaneous fat tissues and 55.1% for muscles (Table 2).

3.3 Gluteus Maximus Muscle Thickness below the Ischial tuberosity

The gluteus maximus muscle deformed the most in the transition from the partially deformed to the undeformed condition. The muscle also deformed while transitioning from the fully deformed to the partially deformed conditions (Figure 3). The mean thicknesses for the partial and fully deformed muscle below the ischial tuberosity (relative to the undeformed thickness) were 70% and 60% respectively.

3.4 Subcutaneous Fat and Skin Thickness below the Ischial tuberosity

Fat tissues below the ischial tuberosity were deformed by a few millimetres while transitioning from the partially deformed to the undeformed state. However, fat thickness below the ischial tuberosity remained almost constant as the buttock transitioned from the fully deformed to the partially deformed states (Figure 3). The thickness of the subcutaneous fat tissue layer below the ischial tuberosity in the partially deformed and fully deformed states (relative to the undeformed thickness) were 81.1% and 80% respectively.

3.5 Gluteus Maximus Muscle Thickness below the Greater Trochanter

On average, the thickness of the gluteus maximus muscle below the greater trochanter remained unchanged when the first block was removed (fully deformed → partially deformed). Muscles also maintained a constant thickness below the greater trochanter when two additional blocks were removed (partially deformed → fully undeformed). The mean (SD) deformation of the gluteus maximus muscle below the greater trochanter from the fully deformed to the partially deformed, and from the partially deformed to the underformed conditions were -0.7 mm (4.0 mm) and 0.2 mm (4.0 mm) respectively.

3.6 Subcutaneous Fat and Skin Thickness below the Greater Trochanter

The thickness of the subcutaneous fat below the greater trochanter gradually increased from the fully deformed to the partially deformed condition and from the partially deformed to the fully undeformed condition. However, the deformations were small (relative to the undeformed thickness), with mean deformations of 1.4 mm (2.6 mm) and 1.1 mm (4.0 mm) for partially deformed and fully deformed conditions respectively.

3.7 Strain Estimates

Tissue strain was defined for the current analysis as the change in the depth of the tissue under each loading conditions relative to the no-load condition. Strains in the gluteus maximus muscle were higher than those in the subcutaneous fat layer. The mean (SD) compressive strain in the gluteus maximus muscle was 33 % (5 %) compared to 16 % (12 %) in the fat tissue layer (Table 3). The subcutaneous fat layer in subjects 6 and 9 was exposed to very small strains. The lowest strains in the gluteus maximus muscle were estimated for subject 5. The CV for the gluteus maximus muscle and subcutaneous fat tissues were 21% and 60% respectively.

4. Discussion

4.1 Soft tissue deformation

Measurements of soft tissue deformation in a semi-recumbent posture were obtained from MRI data for subjects within a broad range of BMI values. The study revealed that muscles below the ischial tuberosity deformed during both phases from weight-bearing to non-weight-bearing, while subcutaneous fat tissues deformed only from weight-bearing to partial weight-bearing conditions. This behaviour, observed across the entire cohort, suggests that the muscle strain is more sensitive to changes in seat support surface and load distribution than strain in subcutaneous fat. This was confirmed by the higher strains estimated for muscles compared to subcutaneous fat.

In this study, measurements for soft tissue deformation were taken below the ischial tuberosity and the greater trochanter. While soft tissue deformation around the greater trochanter may not be of critical importance to typical sitting postures, it certainly is more important for wheelchair users when their lateral side of the thigh is compressed, or for those spending long duration in a side-lying position. In the semi-recumbent configuration used in this study, soft tissue deformation in the gluteal region below the greater trochanter was small compared to the deformation below the ischial tuberosity. In fact, the thickness of muscle tissues below the greater trochanter remained almost unchanged throughout the entire transition from weight-bearing to non-weight-bearing postures implying no deformation took place. This agrees with measurements reported in previous studies (Makhsous et al., 2008; Silber and Then, 2013; Then et al., 2007) and confirms assumptions (Mehta and Tewari, 2000) about the load distribution for seated subject. In terms of magnitude, our measurements of the gluteus maximus thickness (38.5mm – 58.8 mm) seem to be greater than most of the previous studies (< 30 mm), especially those with data obtained from subjects in an upright sitting posture (Brienza et al., 2017; Call et al., 2017; Sonenblum et al., 2015). This may be due to differences in the subjects' orientation in the MRI scanner. In this study, subjects adopted a semi-recumbent posture, in which the subjects' buttocks and thighs were not aligned with the MRI tube. As a result, the transverse images captured a slightly oblique cross-section of the subjects' buttocks, compared to those which would be captured in typical sitting postures. In addition, the orientation, with respect to gravity may have caused the gluteus maximus muscle to translate/deform so that a greater volume of the muscle is positioned closer to the ischial tuberosity. In contrast, our measurements of soft tissue deformation (muscle < 23.8 mm, fat < 14.2 mm) and of the undeformed subcutaneous fat thickness (14 mm – 39.5 mm) seem to fall within ranges reported in previous studies (fat thickness = 5mm – 45mm ; deformation: muscle < 27 mm, fat < 18.5 mm) (Linder-Ganz et al., 2007; Makhsous et al., 2011; Sonenblum et al., 2013; Todd and Thacker, 1994). Measurements of the soft tissue deformation at the partially deformed state (muscle < 23.7 mm, fat < 11.8 mm) agreed with previous measurements taken for subjects in an upright seated posture on deformable cushions (muscle < 21 mm, fat < 27 mm) (Brienza et al., 2017; Call et al., 2017; Sonenblum et al., 2015).

Previous studies were mostly for subjects that fall within the healthy BMI range. However, comparison with our previous study (Al-Dirini et al., 2015) on a cohort with similar demographics, but in a typical seated posture, shows that, on average, the deformations measured in this study were less than those in our previous study. For example, the gluteus maximus deformation under the ischial tuberosity in the current and the previous studies were 17.4 (4) mm and 22.4 (4) mm, respectively. This is not surprising, as the orientation of the body with respect to gravity is expected to influence the magnitude of the compressive load imposed of weight-bearing soft tissues in the gluteal region.

Muscle and fat tissues are known to be almost incompressible (Fung). Hence, the observed deformation is likely due to bulk movement of muscle and fat tissues around, within and between various compartments of connective tissue. It may be that the subcutaneous fat in this area is attached over fairly short distances to the skin, and hence it cannot move very far in response to forces. The behaviour of fat tissues is thought to be analogous to the behaviour of polymer foam under similar loads (Silber and Then, 2013b), where the adipocytes initially deform transversely, until they no longer deform in the same direction (Silber and Then, 2013b). From this point onwards, they start bearing tensile forces (due to the adipocytes pushing against each other), which leads to the observed behaviour (Silber and Then, 2013b). Fat elsewhere on the body might be considerably more mobile.

4.2 Anomalies in the measured soft tissue deformations

Inspection of the subject-specific deformation revealed three anomalies in the measurements obtained. Subject 5 had the largest (negative) change in their pelvic tilt (-13°), which indicates that they lifted their left buttock off the surface of the wooden block. This would have reduced the level of compression on these tissues, which in turn reduced the total tissue deformation (Table 2), with their total soft tissue deformation not exceeding 4.1 mm, which is less than a fifth of the average measured total soft tissue deformation (20.8 mm) in the study cohort. Negative deformation was also noted for the subcutaneous fat layer measured below the ischial tuberosity for five subjects during the transition from fully deformed to the partially deformed conditions. These negative deformations imply an increase in the planar thickness of subcutaneous fat tissues. Also, the combined muscle and fat tissue deformation was not expected to exceed 10 mm in the first transition, and 20 mm in the second transition, but the deformation for subjects 2 and 3 was greater than 10 mm in the first transition, and greater than 20 mm in the second transition. These anomalies are likely due to the deformation of soft tissues in 3D space (Al-Dirini et al., 2015; Kaplan, 2003; Makhsous et al., 2011) and the incompressibility (Silber and Then, 2013b) of muscle and fat. When muscles below the ischial tuberosity are loaded, they undergo 3D deformations. The negative deformations measured in this study suggest that, similar to muscles, fat tissue deformation consists of three components. Such a deformation appears to push fat tissues away from, or towards (in case of negative deformations) the ischial tuberosity. When fat tissues are pushed away from the ischial tuberosity, their thickness decreases, whereas, when the fat tissues are pushed towards the ischial tuberosity, the thickness of fat tissues increases. A similar deformation can be expected for inter-muscular fat tissues under typical loads in functional sitting situations. When the inter-muscular fat tissues are pushed towards the ischial tuberosity, it forces muscle and/or subcutaneous fat tissues to deform more, resulting in an overall soft tissue deformation that is not only influenced by the indentation of the external surface below the buttock, but also by the internal soft tissue layers below the ischial tuberosity.

4.3 Estimates of the strains in muscle and fat tissues

The estimated strains showed that muscles were under higher strains than subcutaneous fat tissues when exposed to external loads that act in a direction different from the orientation of muscle fibres. This was observed for all subjects. Similar findings were reported in previous studies in the literature (Al-Dirini et al., 2015; Linder-Ganz and Gefen, 2004; Linder-Ganz et al., 2009; Silber and Then, 2013a; Then et al., 2007). The study also showed that there is high variation in the estimated strains for both muscles and subcutaneous fat tissues, with greater variation in the estimated strains for subcutaneous fat tissues. Given the small sample in this study, it was not possible to identify the main factors leading to the observed variability. However previous studies suggested that anthropometry (stature, body mass, etc.) (Gefen, 2012), anatomy (radius of curvature for the ischial tuberosity, muscle-to-fat ratio, etc.) (Gefen, 2008a) and soft tissue material properties (Then et al., 2007) are factors that influence the internal strains.

Findings in this study build on current understanding of the interaction between gluteal soft tissues and body support systems, including wheelchairs and seats. In particular, the observed variability in soft tissue deformation is an important factor to consider for improving current seat and cushion designs.

4.4 Limitations

The study is limited by the small sample size. Also, due to gender differences in posture (Dunk and Callaghan, 2005) and soft tissue properties (Silber and Then, 2013), only adult men were recruited for the study. Nonetheless, this sample is the most diverse (in terms of BMI range) in the literature for which *in vivo* deformation measurements have been made. The results of this study provide insight into the *in vivo* quasi-static deformation of soft tissues in the buttock under sitting loads, which were not studied in previously published research.

Tissue deformations were measured in only one posture that is not representative of typical functional seated postures, although it may be more similar to the reclined posture that hospitalised patients may adopt during the daytime. The average orientation of the pelvis relative to the seat surface was 28^{o} in the transverse plan and 67^{o} in sagittal plane, whereas in typical seated situations the external force is oriented more superiorly. The experiment posture was chosen as the least reclined that could be used in the MRI bore, however, it has also resulted in the load being supported by a region that is slightly posterior to the load-bearing region of the ischial tuberosity during typical seated postures. In addition, the experimental posture was not aligned with gravity, which is expected to reduce compression, and increase the shear component of the force acting on load-bearing soft tissues, compared to typical seated postures. Although the experimental setup may have resulted in reasonable consistency in the pelvic orientation in the axial plane, variation was still noted in measurements taken in the sagittal plane (Table 3). As a result, this may have influenced the inclination and the hip flexion angles for the subjects. Consequently, this has likely resulted in a reduction of tissue compression, compared to a typical seated posture. Further research using open MRI, which allows more controlled replication of typical seated postures, will be useful to determine how differences in loading direction influence the patterns of buttock deformation.

The flat, rigid buttock support surface is also not representative of typical seating environments. The flat support surface constrained the net external deformation to be identical between the ischial tuberosity and the greater trochanter regions, except for differences due to skeletal posture changes. A compliant seating surface would be expected to produce different patterns of deformation, with the design of the seating surface influencing those results. More research is needed using padded support surface to determine how padding design alters the patterns of tissue movement and deformation.

There is little agreement in the literature on what would be the ideal slice thickness, with the MRI slice thickness ranging from 0.6mm (Makhsous et al 2011) to 6mm (Al-Dirini et al (2015) and Call et al (2017)). In this study, we have used relatively large slice thickness (10mm) for the scanning protocol, which may have resulted in the loss of some information describing complex anatomical structures, such as the proximal femur (lesser trochanter, femoral neck, etc). Hence, sagittal scans were also obtained to confirm that this potential loss of information in the transverse scans did not affect the region of interest for this study (ischial tuberosity and greater trochanter). Indeed, inspection of sagittal scans confirmed that the transverse scans were able to capture the inferior most point of the ischial tuberosity and the greater trochanter, and hence transverse scans were considered sufficient for this study.

This study assumes that soft tissue deformation is unaffected by deformation history, such that the transition from weight-bearing to non-weight-bearing postures is the same as the deformation caused by the reverse transition (non-weight-bearing to weight-bearing postures). This assumption does not account for the time and history dependencies of soft tissue behaviour, which can strongly influence the transient and dynamic behaviour of soft tissues under compression (Then et al., 2012; Van Loocke et al., 2008; Van Loocke et al., 2009). However, results from Van Loocke et al (2008) indicate that significant stress-relaxation occurs when deformation is held constant after a compressive ramp, especially within the first hundred seconds of relaxation, however, this diminishes after approximately three to six minutes. In this study, subjects remained (as still as possible) in the same posture for approximately five to six minutes before the scanning to allow history dependencies to fade out.

Future research investigating the *in vivo* behaviour of gluteal soft tissues for seat-human interaction is needed to account for the time dependent component. Using the current protocol, MRI scanning may not provide time-history information about soft tissue deformation required for characterising the viscoelastic material properties. Ultrasound measurements may provide an attractive alternative to describe the time-dependency of the behaviour (Krouskop et al., 1987; Makhsous et al., 2008). A suggested protocol would couple MRI and ultrasound imaging modalities to characterise the 3D quasi-static and the viscoelastic properties of soft tissues under deformations associated with sitting.

5 Conclusion

Muscles gradually deform throughout the entire transition from weight-bearing to non-weight-bearing conditions, while subcutaneous fat deformed little after the first transition from non-weight-bearing to partial-weight-bearing conditions. This suggests that the muscle strain will be more sensitive to changes in seat support surface load and load distribution than strain in subcutaneous fat.

Acknowledgment

The research was funded by the AutoCRC and the Maurice de Rohan Scholarship.

References

1. Stockton, L. and D. Parker, Pressure relief behaviour and the prevention of pressure ulcers in wheelchair users in the community. Journal of tissue viability, 2002. 12(3): p. 84, 88-90.

2. Wall, J., Preventing pressure sores among wheelchair users. Professional nurse, 2000. 15(5): p. 321-324.

3. Shabshin, N., et al., Use of weight-bearing MRI for evaluating wheelchair cushions based on internal soft-tissue deformations under ischial tuberosities. Journal of rehabilitation research and development, 2010. 47(1): p. 31-42.

4. Linder-Ganz, E., et al., Assessment of mechanical conditions in sub-dermal tissues during sitting: a combined experimental-MRI and finite element approach. Journal of biomechanics, 2007. 40(7): p. 1443-1454.

5. Untaroiu, C., et al. Characterization of the lower limb soft tissues in pedestrian finite element models. in 19th International Technical Conference on the Enhanced Safety of Vehicles. 2005.

6. Untaroiu, C.D. and Y.-C. Lu, Material characterization of liver parenchyma using specimen-specific finite element models. Journal of the mechanical behavior of biomedical materials, 2013. 26: p. 11-22.

7. Gefen, A., How much time does it take to get a pressure ulcer? Integrated evidence from human, animal, and in vitro studies. Ostomy wound management, 2008. 54(10).

8. Linder-Ganz, E., et al., Pressure–time cell death threshold for albino rat skeletal muscles as related to pressure sore biomechanics. Journal of biomechanics, 2006. 39(14): p. 2725-2732.

9. Linder-Ganz, E. and A. Gefen, Mechanical compression-induced pressure sores in rat hindlimb: muscle stiffness, histology, and computational models. Journal of Applied Physiology, 2004. 96(6): p. 2034-2049.

10. Makhsous, M. and F. Lin, A Finite-Element Biomechanical Model for Evaluating Buttock Tissue Loads in Seated Individuals with Spinal Cord Injury, in Bioengineering Research of Chronic Wounds. 2009, Springer. p. 181-205.

11. Salcido, R., A. Popescu, and C. Ahn, Animal models in pressure ulcer research. The journal of spinal cord medicine, 2007. 30(2): p. 107-116.

12. Makhsous, M., et al., Investigation of soft-tissue stiffness alteration in denervated human tissue using an ultrasound indentation system. The journal of spinal cord medicine, 2008. 31(1): p. 88-96.

13. Vannah, W.M. and D.S. Childress, Indentor tests and finite element modeling of bulk muscular tissue in vivo. Journal of rehabilitation research and development, 1996. 33: p. 239-252.

14. Makhsous, M., et al., Use of MRI images to measure tissue thickness over the ischial tuberosity at different hip flexion. Clinical Anatomy, 2011. 24(5): p. 638-645.

15. Todd, B.A. and J.G. Thacker, Three-dimensional computer model of the human buttocks, in vivo. Journal of rehabilitation research and development, 1994. 31: p. 111-111.

16. Then, C., et al., A method for a mechanical characterisation of human gluteal tissue. Technology and Health Care, 2007. 15(6): p. 385-398.

17. Makhsous, M., et al., Finite element analysis for evaluation of pressure ulcer on the buttock: development and validation. IEEE Transactions on Neural Systems and Rehabilitation Engineering, 2007. 15(4): p. 517-525.

18. Sonenblum, S.E., et al., 3-dimensional buttocks response to sitting: A case report. Journal of tissue viability, 2013. 22(1): p. 12-18.

19. Linder-Ganz, E. and A. Gefen, The effects of pressure and shear on capillary closure in the microstructure of skeletal muscles. Annals of biomedical engineering, 2007. 35(12): p. 2095-2107.

20. Al-Dirini, R.M., M.P. Reed, and D. Thewlis, Deformation of the gluteal soft tissues during sitting. Clinical Biomechanics, 2015.

21. Brienza, D., Vallely, J., Karg, P., Akins, J., Gefen, A., 2017. An MRI investigation of the effects of user anatomy and wheelchair cushion type on tissue deformation. Journal of Tissue Viability.

22. Call, E., Hetzel, T., McLean, C., Burton, J.N., Oberg, C., 2017. Off loading wheelchair cushion provides best case reduction in tissue deformation as indicated by MRI. Journal of Tissue Viability.

23. Sonenblum, S.E., Sprigle, S.H., Cathcart, J.M., Winder, R.J., 2015. 3D anatomy and deformation of the seated buttocks. Journal of tissue viability 24, 51-61.

24. Silber, G. and C. Then, Preventive biomechanics. 2013: Springer.

25. Silber, G. and C. Then, Human Body Models: Boss-Models, in Preventive Biomechanics. 2013, Springer. p. 175-244.

26. Mehta, C. and V. Tewari, Seating discomfort for tractor operators–a critical review. International Journal of Industrial Ergonomics, 2000. 25(6): p. 661-674.

27. Kaplan, R.J., Physical Medicine and Rehabilitation: Pearls of Wisdom. 2003: Boston Medical Publishing.

28. Linder-Ganz, E., et al., Real-time finite element monitoring of sub-dermal tissue stresses in individuals with spinal cord injury: toward prevention of pressure ulcers. Annals of biomedical engineering, 2009. 37(2): p. 387-400.

29. Gefen, A., Usage of Anthropometry to Determine Etiological and Risk Factors in Deep-Tissue Injury, in Handbook of Anthropometry. 2012, Springer. p. 2443-2457.

30. Gefen, A., The Compression Intensity Index: A practical anatomical estimate of the biomechanical risk for a deep tissue injury. Technology and Health Care, 2008. 16(2): p. 141-149.

31. Then, C., T. Vogl, and G. Silber, Method for characterizing viscoelasticity of human gluteal tissue. Journal of biomechanics, 2012. 45(7): p. 1252-1258.

32. Van Loocke, M., C. Simms, and C. Lyons, Viscoelastic properties of passive skeletal muscle in compression—Cyclic behaviour. Journal of biomechanics, 2009. 42(8): p. 1038-1048.

33. Van Loocke, M., C. Lyons, and C. Simms, Viscoelastic properties of passive skeletal muscle in compression: stress-relaxation behaviour and constitutive modelling. Journal of biomechanics, 2008. 41(7): p. 1555-1566.

34. Krouskop, T., D. Dougherty, and F. Vinson, A pulsed Doppler ultrasonic system for making noninvasive measurements of the mechanical properties of soft tissue. Journal of rehabilitation research and development, 1987. 24(2): p. 1-8.

Figure 1: This figure shows an illustration (a) and a photograph (b) of the setup for MRI scanning. Figure (c) shows the wooden board (dark colour) with removable inserts (light colour). The inserts were removed from underneath the left buttock of each subject to alter the boundary condition imposed on the buttock during each of the MRI scanning stages. The different loading conditions were (1) fully deformed (MRI of the buttocks in this condition is shown in (d)), (2) Partially deformed (shown in e) and (3) fully undeformed (f).

Figure 2: (a) an illustration of tissue thicknesses measured from MRI scans. In this slice, the gluteus maximus muscle thickness below the ischial tuberosity and the greater trochanter are indicated by numbers 1 and 3, respectively. The fat thickness below the ischial tuberosity and the greater trochanter are indicated by numbers 2 and 4, respectively. Figure (b) shows the pelvic tilt angle (ϴ), relative to the seat surface (shown as the blue rectangle below the pelvis). Figures (c) and (d) show the pelvic orientation, with respect to the seat surface in the sagittal (β) and transverse (Φ) planes, respectively.

Figure 3: Measurements of soft tissue thickness below the ischial tuberosity (left) and the greater trochanter (right) for each of the three different loading conditions. It appears that the gluteus maximus muscle below the ischial tuberosity continued to deform throughout the entire load range, while fat seemed to block after the first transition. The thickness of the gluteus maximus muscle seems to remain constant throughout the entire load range.

Table 1: Summary of the study cohort demographics.

Table 2: Summary of soft tissue deformations measured below the ischial tuberosity of each subject for each of the transitions.

Table 3: Summary of Pelvic tilt and orientation, and Green-Lagrange (GL) strains in muscles and fat tissues below the ischial tuberosity estimated from MRI scans for each subject.

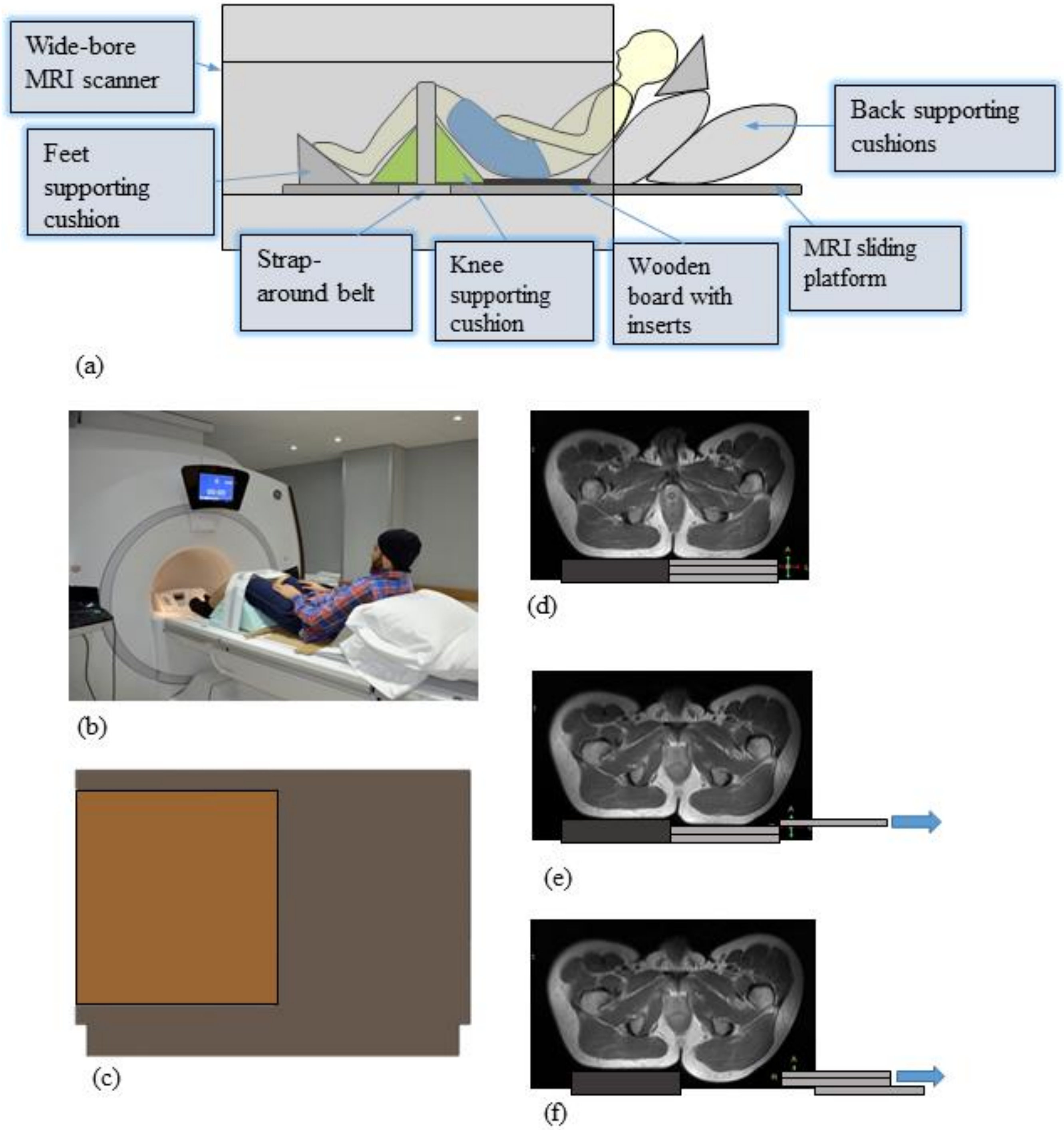
Wide-bore MRI scanner
Feet supporting cushion
Strap-around belt
Knee supporting cushion
Wooden board with inserts
MRI sliding platform
Back supporting cushions
(a)
(b)
(c)
(d)
(e)
(f)

Figure 1

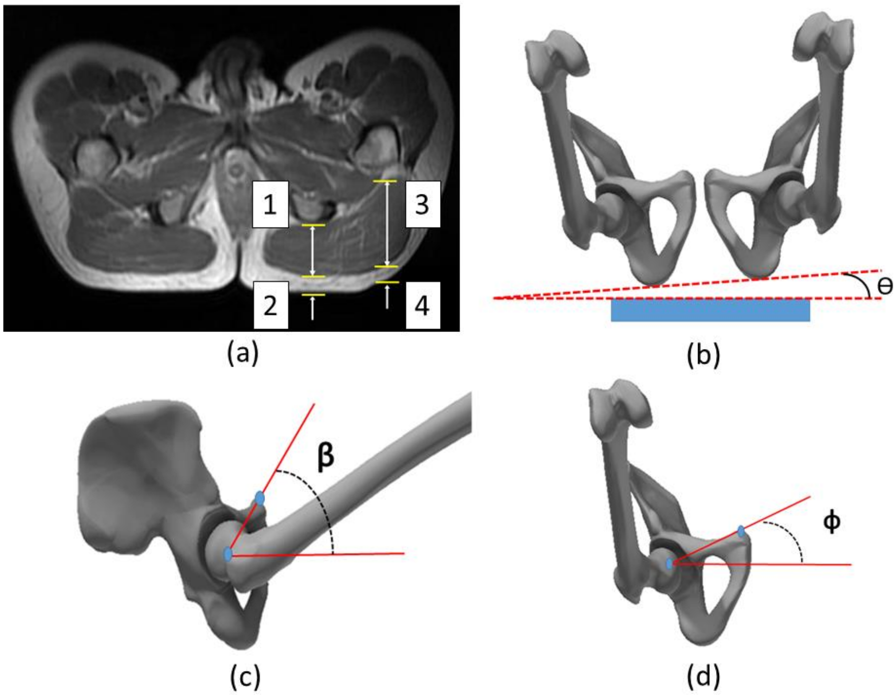

Figure 2

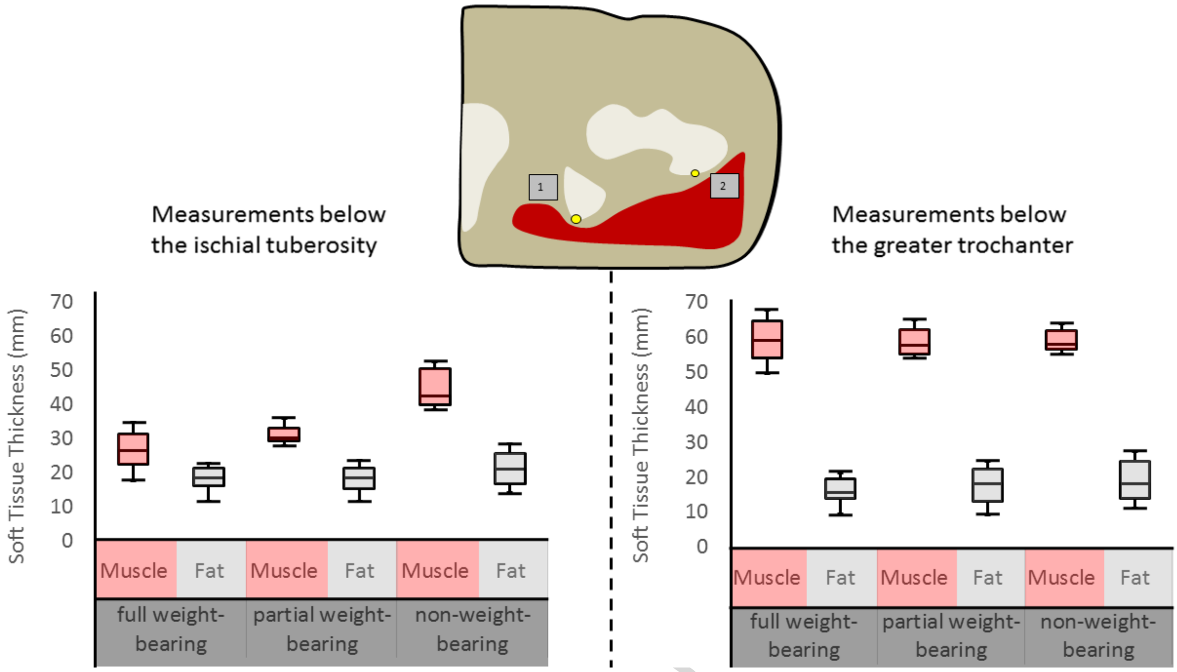

1
2
Measurements below the ischial tuberosity
Measurements below the greater trochanter
Soft Tissue Thickness (mm)
70
60
50
40
30
20
10
0
Muscle
Fat
Muscle
Fat
Muscle
Fat
full weight-bearing
partial weight-bearing
non-weight-bearing
Soft Tissue Thickness (mm)
70
60
50
40
30
20
10
0
Muscle
Fat
Muscle
Fat
Muscle
Fat
full weight-bearing
partial weight-bearing
non-weight-bearing

Figure 3

Table 1

Subject	BMI ($kg.m^{-2}$)	Body mass (kg)	Stature (cm)	Age (years)
1	24.2	79.2	169.4	39
2	28.4	80.7	180.8	33
3	35.6	110.8	180.8	30
4	26.1	84.6	175.6	31
5	25.9	79.8	180.0	25
6	25.0	81.6	170.0	31
7	26.6	76.9	168.6	19
8	35.7	115.5	181.7	29
9	31.0	102.4	176.4	27
10	21.7	62.3	179.9	31

Table 2

Subject Measurements					Deformation Partially deformed → Undeformed 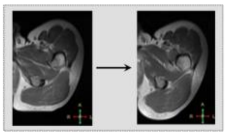		Deformation Fully deformed → partially deformed 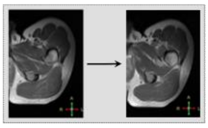		Total Deformation Fully deformed → Undeformed 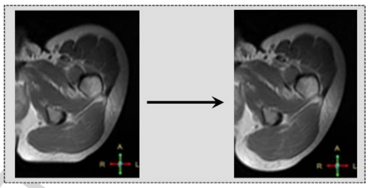				
ID	**BMI (kgm^{-2})**	**Stature (cm)**	**Undeformed Thickness (mm) Muscle**	**Undeformed Thickness (mm) Fat**	**Muscle (mm)**	**Fat (mm)**	**Muscle (mm)**	**Fat (mm)**	**Muscle (mm)**	**Fat (mm)**	**Muscle +Fat (mm)**	**Muscle (%)^**	**Fat (%)^**
1	24.2	180.8	39.3	14.0	10.7	1.1	10.9	1.3	21.6	2.4	24.0	55.1	17.3
2	28.4	168.6	44.1	33.1	16.1	11.3	6.1	0.4	22.2	11.7	33.9	50.4	35.3
3	35.6	176.4	41.1	39.5	11.3	11.8	6.3	2.4	17.6	14.2	31.8	42.9	36.0
4	26.1	180	43.4	24.7	9.8	2.0	3.7	4.3	13.5	6.3	19.8	31.1	25.7
5	25.9	180.0	39.5	15.4	9.3	-2.6	-1.6	-0.6	7.7	-3.6	4.1	19.3	-20.6
6	25.0	180.8	52.8	21.4	23.7	2.9	0.1	-3.5	23.8	-0.6	23.2	45.0	-2.6
7	26.6	170	38.5	25.8	7.4	6.4	7.0	1.3	14.4	7.7	22.1	37.5	29.8
8*	35.7	179.9	58.8	16.5	9.2	5.0	7.4	-2.7	16.6	2.3	18.9	28.3	14.1
9**	31.0	181.7	41.3	20.6	11.1	2.2	8.6	-6.7	18.7	-4.5	14.2	47.7	0.0
10	21.7	169.4	54.3	17.5	11.5	2.7	7.9	-0.5	14.2	2.2	16.4	35.7	12.6

^ Percentage of total soft tissue deformation
* Subject had fat infiltrating into the Gluteus Maximus muscle
** Subject's buttock was slightly deformed in the undeformed scans

Note: negative deformations indicate an increase in tissue thickness, while positive deformations indicate a decrease in thickness at the measurement site.

Table 3

ID	Change in pelvic tilt ^		Pelvis orientation		Strain	
	Partial weight-bearing (º)	Non-weight bearing (º)	Axial angle (º)	Sagittal angle (º)	$\varepsilon_{muscle\ (GL)}$ (%)	$\varepsilon_{fat\ (GL)}$ (%)
1	-6.8	-7.8	32.8	52.8	40	16
2	2.1	-5.3	***N/A***	***N/A***	38	29
3	-2.4	0.2	29.8	67.9	34	30
4	-0.6	-2.6	28.4	88.7	26	22
5	-5.2	-13.1	29.9	56.6	20	20
6	-5.5	-1.2	23.0	72.8	35	3
7	1.4	0.1	26.3	53.7	30	25
8*	-0.1	-0.1	29.2	69.7	24	13
9**	-1.3	-0.2	24.8	73.0	36	0
10	-0.4	1.5	31.8	58.2	29	12

^ Percentage of total soft tissue deformation

* Subject had fat infiltrating into the Gluteus Maximus muscle

** Subject's buttock was slightly deformed in the undeformed scans

Note: negative de
thickness, while p
in thickness at the

* Subject had fat infiltrating into the Gluteus Maximus muscle.

** Subject's buttock was slightly deformed in the non-weight-bearing scans.

^ Relative to the full-weight-bearing condition.

N/A High distortion in the MRI scans near the femoral head and the public symphasis.

Highlights

- Gluteal tissue deformation under a range of loads were measured for a diverse cohort using MRI scans.
- Muscles deformed throughout the transition from weight-bearing to non-weight-bearing conditions.
- Subcutaneous fat deformed little beyond the partial-weight-bearing condition